Characterization of Platinum(II)–Phosphato Complexes of Uridine Nucleotides

Rathindra N. Bose,* Lori L. Slavin,† Jeff W. Cameron,‡ Donna L. Luellen,‡ and Ronald E. Viola§

Department of Chemistry, Kent State University, Kent, Ohio 44240

Received October 6, 1992

Reactions of uridine 5′-di- and -triphosphates with *cis*-diamminedichloroplatinum(II) at or near neutral pH yielded substantial phosphato chelates. Each nucleotide afforded a pair of diastereomers due to the creation of an asymmetric center at the α- and β-phosphorus atoms of the UDP and UTP upon complexation to platinum(II). In addition to the phosphato complexes, nitrogen (N(3)) bound complexes are also formed. Further, secondary reaction of these pyrimidine base bound complexes resulted in platinum blue (for UDP) and purple (for UTP) complexes as minor products. Diastereomers are separated by reversed phase HPLC method and characterized by one- and two-dimensional phosphorus-31 NMR and CD spectroscopic methods. The phosphorus atoms of the coordinated phosphate groups exhibit 8–12 ppm coordination chemical shifts. For the UDP complexes, distinct ^{31}P resonances for each diastereomer were observed. The coordinated γ-phosphate of UTP diastereomers exhibited a broad multiplet while the β-phosphate group showed distinct doublets of doublet. The CD spectra of the UDP diastereomers displayed opposite Cotton effects at 300 nm while both complexes exhibited a positive Cotton effect at 260 nm. Once separated, these diastereomers slowly ($t_{1/2} = 25 \pm 5$) redistribute to a mixture of two with almost equal abundance. Kinetic studies based on HPLC and ^{31}P NMR measurements point to a mechanism in which the isomerization proceeds through a rate limiting ring-opening. When the chelate ring is opened, deligation and phosphate hydrolysis can also occur, resulting in free UDP, UMP, and orthophosphate bound to platinum.

Introduction

Platinum(II)–nucleotide chemistry[1–4] has received a great deal of attention recently, due to the antineoplastic activity of *cis*-diamminedichloroplatinum(II) (*cis*-DDP). The biochemistry of this square planar complex has been almost exclusively centered around the binding of purine nucleotides through the nitrogen donor sites.[1–4] Direct covalent bonding through the phosphate moiety of nucleotides to platinum(II) has not been explored in detail.[5–7] Metal–phosphate interactions play an important role in many key enzyme reactions ranging from phosphokinases to DNA polymerases.[8–12] Several inert metal complexes such as Cr(III), Co(III), Rh(III), etc. have been used to mimic the role of metal ions in hydrolytic cleavage of the phosphate chains in some enzyme-catalyzed reactions.[11,13] Platinum(II) phosphates may serve as better models, since the coordinated water molecules are more acidic and the ambiguities related to the intramolecular vs intermolecular hydroxyl transfer reactions can be eliminated. Futhermore, the metal ions in enzymatic reactions are dicationic and platinum(II) would mimic this charge requirement, which is important since the hydrolysis is greatly influenced by the charge of the metal centers. Although platinum(II) offers square planar geometry as compared to the octahedral stereochemistry of biological metal ions, such a difference in geometric feature does not appear to significantly influence the hydrolytic cleavages of phosphate esters and diesters. Here we report the kinetics of formation and isomerization of phosphato complexes of uridine 5′-di- and -triphosphates to platinum(II), along with the HPLC, CD, and one- and two-dimensional NMR characterization of the resulting products.

Experimental Section

Materials. Uridine 5′-di- and -triphosphates (UDP and UTP), D_2O (99% atom), NaOD, DNO_3 (Sigma), NaH_2PO_4, Na_2HPO_4, sodium acetate, formic acid (Aldrich), and acetic acid (Fisher Scientific) were used without further purification. *cis*-Diamminedichloroplatinum(II) was prepared by following the method of Dhara.[14] $NaClO_4$ was prepared by neutralization of Na_2CO_3 with perchloric acid. Buffers of desired pH values were prepared by mixing the appropriate concentrations of acids and their conjugate bases.

Physical Measurements. NMR Measurements. Nuclear magnetic resonance experiments were performed either on a 300-MHz GE or a 400-MHz Varian instrument equipped with variable-temperature probes. The chemical shifts for ^{31}P and proton resonances are with respect to 85% phosphoric acid at 0.0 ppm and the H–O–D signal at 4.67 ppm. Typical ^{31}P spectra were obtained by selecting 4000–10000-Hz frequency windows, 25-μs pulse width, 1-s pulse repetition delay, 8–16K data points, and 200–500-ms acquisition time. A line-broadening factor of 2 Hz was introduced before the Fourier transformation. Occasionally, much longer delays for pulse repetitions were used in order to ascertain that no signals remained undetected. Two-dimensional COSY experiments were performed using sweep widths of 2000–4000 Hz with 512 × 512 matrices. The usual pulse sequence, $\pi/2-t_1-\pi/2-a_t$ (t_1 and a_t are the evolution and acquisition times), was followed. A Gaussian line-broadening factor of 3 Hz was utilized before generating two-dimensional contour plots.

* To whom correspondence should be addressed.

† Present address: Department of Chemistry, Austin Peay State University, Clarksville, TN 37044.

‡ Undergraduate participants.

§ Department of Chemistry, University of Akron, Akron, OH 44325.

(1) Sherman, S. E.; Lippard, S. J. *Chem. Rev.* **1987**, *87*, 1153.
(2) Reedijk, J.; Fichtinger-Schepman, A. M. J.; VanDosterom, A. T.; VandePutte, P. *Struct. Bonding (Berlin)* **1987**, *67*, 53.
(3) Kline, T. P.; Live, D.; Zon, G.; Marzilli, L. G. *J. Am. Chem. Soc.* **1989**, *111*, 7057.
(4) Goswami, N.; Bennett-Slavin, L. L.; Bose, R. N. *J. Chem. Soc., Chem. Commun.* **1989**, 432.
(5) Slavin, L. L.; Bose, R. N. *J. Chem. Soc., Chem. Commun.* **1990**, 1256.
(6) Reily, M. D.; Hambley, T. W.; Marzilli, L. G. *J. Am. Chem. Soc.* **1988**, *110*, 2999; Reily, M. D.; Marzilli, L. G. *J. Am. Chem. Soc.* **1986**, *108*, 8299.
(7) Louie, S.; Bau, R. *J. Am. Chem. Soc.* **1987**, *99*, 3874.
(8) Qian, L.; Sun, Z.; Gao, J.; Movassagh, B.; Morales, L.; Bowman Mertes, K. *J. Coord. Chem.* **1991**, *23*, 155; Mertes, M. P.; Bowman Mertes, K. *Acc. Chem. Res.* **1990**, *23*, 413.
(9) Hendry, P.; Sargeson, A. M. In *Progress in Inorganic Chemistry*: Bioinorganic Chemistry; Lippard, S. J. Ed.; John Wiley and Sons, Inc.: New York, 1990.
(10) Rawji, G. H.; Milburn, R. M. *Inorg. Chim. Acta* **1988**, *150*, 227. Rawji, G.; Hediger, M.; Milburn, R. M. *Inorg. Chim. Acta* **1983**, *79*, 247. Tafesse, F.; Massoud, S. S.; Milburn, R. M. *Inorg. Chem.* **1985**, *24*, 2591.
(11) Cornelius, R. D.; Cleland, W. W. *Biochemistry* **1978**, *17*, 3279; Norman, P. R.; Cornelius, R. D. *J. Am. Chem. Soc.* **1982**, *104*, 2356; Reibenspies, J.; Cornelius, R. D. *Inorg. Chem.* **1984**, *23*, 1563.
(12) Kramer, P.; Nowak, T. *J. Inorg. Biochem.* **1988**, *32*, 135.
(13) Lue, Z.; Shorter, A. L.; Lin, I.; Dunaway-Mariano, D. In *Mechanisms of Enzymatic Reactions: Stereochemistry*; Frey, P. A., Ed.; Elsevier: New York, 1985.
(14) Dhara, S. C. *Indian J. Chem.* **1970**, *8*, 193.

0020-1669/93/1332-1795$04.00/0 © 1993 American Chemical Society

Solutions were typically prepared using stock solutions of *cis*-platin and nucleotide. Reaction mixtures were prepared by mixing *cis*-platin (5–8 mM) with the nucleotide in excess (10–20 mM) and adjusted to pH 6.4–7.0. Solutions were thermostated at 40 °C for 24 h. During the reaction, the pH dropped slightly but was readjusted to its initial value after 24 h. Aliquots were taken from the reaction mixtures, and NMR spectra were recorded at the desired time intervals. For most kinetic experiments, reaction mixtures were immediately placed in the 10-mm probe, which had been preequilibrated to 40 °C. Reactions were monitored for 20 h, utilizing 15-min or longer time intervals between data acquisitions.

HPLC Separations. The products of the reactions were separated by HPLC methods utilizing reversed phase C-18 columns on a ternary gradient ISCO system, interfaced with an IBM PS/2 computer. Phosphate (pH 6.8), acetate (pH 5.2), and formate (pH 3.8) buffers were used as mobile phases, and a flow rate of 1 mL/min was used. Reaction mixtures were prepared from stock solutions using equal molar ratios, or ratios with the nucleotide in excess, and adjusted to pH 7.0. Solutions were thermostated at 40 °C for 24 h and then readjusted to pH 7.0. Aliquots from the reaction mixture were injected, and the fractions were detected at 254 or 260 nm by an UV–vis detector.

Rate Measurements. The rates of formation of various nucleotide complexes were monitored either on a double-beam UV–vis spectrophotometer (Perkin Elmer Lambda 600 or Varian DMS 100; interfaced with a Epson Equity 1^+ computer) or by following the change in intensity of specific ^{31}P NMR signals with time. The reactions were carried out with excess nucleotide over the platinum complex while maintaining a constant ionic strength of 0.5 M with $NaClO_4$. For the UV–vis measurements nucleotides were present in at least 10-fold excess while for the NMR experiments nucleotide concentrations exceeded that of the platinum complex only 2–4-fold. When the reaction was followed at 375 nm, an initial decrease in absorbance was observed, followed by a slow increase for up to 21 days. The absorbance change was recorded every 10 min initially (for up to 12 h), and then at 6–12-h intervals. The absorbance time data can be described by the biphasic expression

$$D - D_\infty = ae^{-k_0 t} + be^{-k_1 t} \quad (1)$$

where D and D_∞ represent the absorbance at time t and at the end of the reaction and k_0 and k_1 are the first-order rate constants. The extinction coefficient of the intermediate can be estimated from the values of the preexponential constants, a and b.

The rate constants for the formation of phosphato complexes were estimated from the intensity–time data of ^{31}P resonances. Plots of the intensity of ^{31}P resonances of the products vs time feature an exponential growth. The rate constants were evaluated by solving the expression

$$I_t = (I_0 - I_\infty)e^{-k_0 t} + I_\infty \quad (2)$$

where I_t is the normalized intensity of a specific product signal at any time, I_0 is the intensity at the beginning of the reaction, and I_∞ is the limiting intensity at infinite time. The normalized intensity was obtained by equating the sum of the intensity for the signals for each of the products to unity, and then calculating the fraction of the intensity for each of the desired product signals.

The half-lives of isomerization were estimated from the area under desired peaks in the HPLC chromatograms. Here again, the areas under peaks were normalized and half-lives were estimated from the normalized area vs time data.

Circular Dichroism Measurements. Spectra were obtained on a Jasco J-500A instrument interfaced with a Samsung computer. The ellipticity values were calibrated[15] with ammonium *d*-camphor-10-sulfonate at 280 nm. The molar ellipticity values of the phosphato diastereomers were estimated in the following manner. The concentrations of each peak representing the phosphato complex, which were collected from the HPLC experiments, were estimated spectrophotometrically. First, the molar absorptivity value (1.06×10^4 M^{-1} cm^{-1}) was determined for the free UDP in phosphate buffer at 260 nm. The UV–vis spectra recorded for each fraction also exhibited a band at 260 nm. The concentration for each eluant was then determined by utilizing the molar absorptivity value for free UDP with the assumption that the 260-nm band, which arises from the heterocyclic base moiety of the nucleotide, was not significantly affected by metal complexation to the phosphate group. From the CD spectra, the molar ellipticity values for each fragment were calculated using the expression

$$[\theta] = \frac{10^2\theta}{cl} \quad (3)$$

where $[\theta]$ and θ represent the molar ellipticity and the measured ellipticity in degrees, respectively. Concentration, c, has units of mol L^{-1} and the path length, l, units are in cm.

Estimation of Acidity Constants. The acidity constants for the phosphato complexes were evaluated from the ^{31}P chemical shift vs pH data. All of these complexes exhibit monoprotic acidic behavior in the pH range from 2 to 10. A nonlinear least-squares computer fit of the chemical shift–pH data according to eq 4 readily afforded the acid dissociation constants (K_a).[16,17]

$$\delta = \delta_1 f_1 + \delta_2 f_2 = \frac{\delta_1[H_3O^+] + \delta_2 K_a}{K_a + [H_3O^+]} \quad (4)$$

In this equation, δ_1 and δ_2 are the chemical shifts of the protonated and deprotonated forms, and f_1 and f_2 are the fractions of the two forms present at a given pH ($f_1 + f_2 = 1.0$). It was not possible to quantitate the spectra of these complexes below pH 2, due to the rapid deligation of the phosphato complexes.

Results

Reaction of UDP with *cis*-DDP. The reaction of UDP with *cis*-DDP was followed by phosphorus-31 NMR, proton NMR, and UV–vis spectroscopy. Figure 1a shows the phosphorus-31 NMR spectra of the UDP (8 mM)-*cis*-DDP (20 mM) reaction mixture recorded at various time intervals. The two doublets at −6.17 (J = 22.2 Hz) and −8.69 (J = 22.1 Hz) ppm are for the β- and the α-phosphate groups in the free nucleotide. As the reaction proceeds, two new sets of doublets are formed at about 10 ppm downfield with respect to the doublets of the free UDP. No further changes in the signal intensity of these downfield signals were apparent after 20 h. Figure 1b exhibits the COSY spectra of the reaction mixture which were recorded after 24 h, when no further changes in the ^{31}P resonances were observed. The spectra reveal the connectivity among the new sets of doublets (C and D), as well as those between the initial doublets (A and B). The new signals are due to the formation of phosphato chelates. The formation of monodentate complexes through α- and β-phosphate coordinations can be ruled out from the coordination chemical shifts and correlation spectroscopy. For example, a monodentate complex with coordinated β-phosphate should exhibit a downfield chemical shift of the bound phosphate group, with little or no effect on the shift of the α-phosphate moiety. Therefore, a connectivity between one of the downfield doublets (C or D) and the doublet of the of the α-phosphate group (B) would be expected. A phosphato chelate coordinating through the α- and β-phosphate groups will create an asymmetric center at the former phosphate group, and two diastereomers will result. Two sets of doublets under each of C and D, along with the HPLC separation and CD data (vide infra), are consistent with such formation of diasteromeric chelates. The chemical shifts of the chelates as a function of pH are listed in Table I.

Although the phosphorus resonance intensities did not change after 20 h, nor did new peaks appear in the spectra, the changes in the proton NMR spectrum were observed to occur in two distinct phases. The first phase of these changes is in parallel with the formation of these new ^{31}P resonances. The second phase of the reactions was much slower. For example, in the proton NMR spectra for the UDP reaction at pH 6.4, two doublets at 8.14 ppm (J = 8.4 Hz) and 6.17 ppm appear as shoulders on the free H(6) and H(5) doublets of uracil at 8.09 ppm (J = 8.1

(15) Cassim, J. Y.; Yang, J. T. *Biochemistry* **1969**, *8*, 1947.

(16) Slavin, L. L.; Bose, R. N. *J. Inorg. Biochem.* **1990**, *40*, 339.

(17) (a) Bose, R. N.; Goswami, N.; Moghaddas, S. *Inorg. Chem.* **1990**, *24*, 3461. (b) Bose, R. N.; Viola, R. E.; Cornelius, R. *J. Am. Chem. Soc.* **1984**, *106*, 3336.

(18) Glasgoe, P. K.; Lang, F. A. *J. Phys. Chem.* **1960**, *64*, 188.

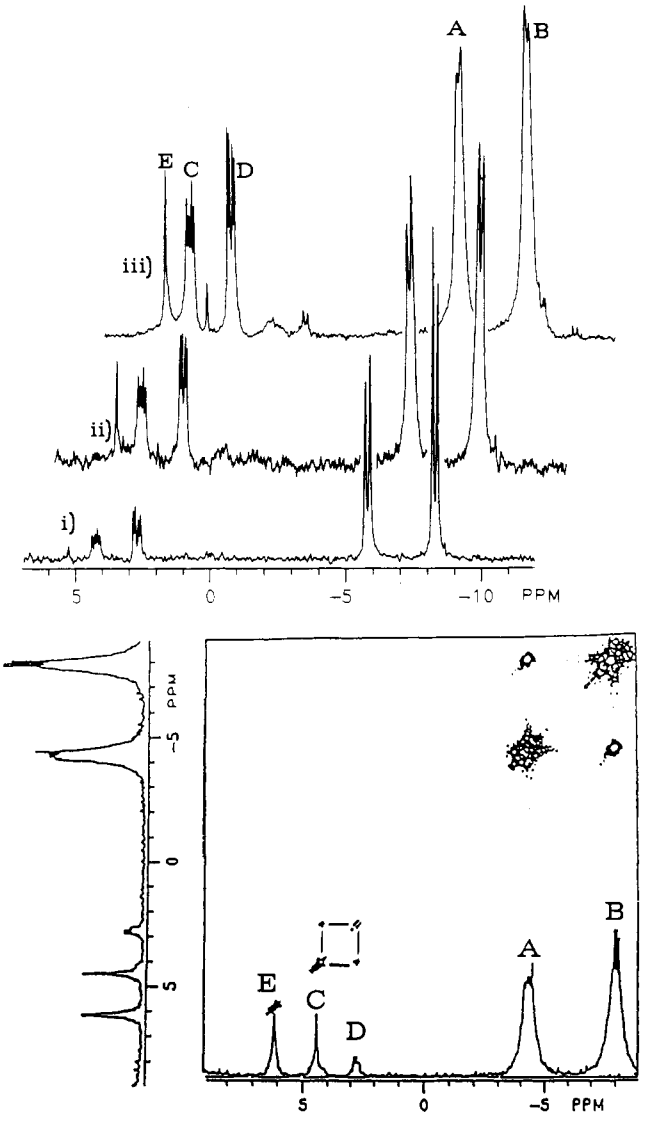

Figure 1. (a) Top: 126.5-MHz phosphorus-31 NMR spectrum of *cis*-platin (8.0 mM) and UDP (20 mM) at pH 6.8 recorded after (i) 2 h, (ii) 10 h, and (iii) 7 days. Peaks A and B are for β- and α-phosphates of free UDP and for the nitrogen bound complexes; peaks C and D are for β- and α-phosphates of phosphato complexes, and peak E is for UMP. (b) Bottom: Two-dimensional ^{31}P spectra (COSY) of the reaction mixture as in Figure 1a at pH 7.0. Solid lines are drawn in the 2D-contours to indicate connectivity between peaks C and D. Similar connectivity is observed between peaks A and B. The resolution of the spectra has diminished due to the selection of 512 × 512 matrix.

Hz) and 6.10 ppm (J = 8.1 Hz) during the first 20 h of the reaction (Figure 2). At higher pH, the two doublets move downfield and appear as distinct peaks, while at lower pH the resonances move upfield and are masked under the free H(6) and H(5) doublets of uracil. In the second phase, multiplets at 7.89 and 5.95 ppm slowly appeared. The secondary changes in the proton resonances are also accompanied by the appearance of a blue color.

The new signals observed for the H(6) and H(5) protons are indicative of the formation of nitrogen bound complexes, since remote phosphate complexation should exert very little or no influence on the chemical shifts of the base protons. Therefore, in addition to the formation of phosphato complexes in the initial phase of the reaction, nitrogen-coordinated products are also formed. The coordination chemical shifts for the H(6) and H(5) protons are small. Such small coordination chemical shifts are consistent with N(3) coordination since these protons are not adjacent to the coordination site.[5]

The reaction was also followed spectrophotometrically at 300 and 375 nm at 40 °C. At 300 nm a monotonic increase in absorbance was observed, while at 375 nm an initial decrease during the first 10–12 h, followed by an increase in absorbance for up to 15 days, was encountered due to the formation of blue products. Rate constants evaluated from absorbance–time traces are listed in Table II. A good agreement is apparent between rate constants obtained from ^{31}P intensity measurements and k_0 evaluated from biphasic profiles.

The blue product exihibits an absorption band centered around 600 nm. The extent of the blue complex formation depends on the concentrations of platinum and nucleotide and on pH. An absorbance value of 0.36 was recorded after 14 days utilizing a reaction mixture of 8.0 mM each in UDP and *cis*-DDP at pH 6.5. During the same time, when the UDP concentration was doubled while keeping [Pt] invariant, the absorbance value was found to be 0.26. At pH 3.0 the reaction mixture containing 8.0 mM each *cis*-DDP and nucleotide afforded an absorbance value of 0.12 while at pH >8.5 no blue product formation was apparent. The highest absorbance for this reaction mixture was recorded to be 0.42 at pH 5.0. Furthermore, when platinum concentration was doubled keeping [nucleotide] constant at 8.0 mM, the absorbance value was decreased to 0.32. Several attempts to separate these blue products from the phosphato complexes and the free nucleotide utilizing gel-filtration and anion exchange chromatography were unsuccessful. Invariably, the blue complexes were found to decompose in the column. Although these complexes were separated by C-18 reversed phase HPLC method utilizing

Table I. Phosphorus-31 Chemical Shifts (Coupling Constants in Hz) of Pt(II)–UDP Phosphato Complexes as a Function of pH

	chem shifts, ppm	
pH[a]	β-phosphate	α-phosphate
1.91	2.85[b]	2.15[b]
	2.85	2.15
2.50	3.15[b]	2.35[b]
	3.10	2.16
3.36	4.27 (22.1)[c]	2.90 (21.8)[c]
	4.16 (19.4)	2.80 (23.2)
4.40	4.49 (24.4)	2.29 (23.2)
	4.41 (22.5)	2.91 (23.6)
5.45	4.53 (23.1)	3.00 (23.0)
	4.43 (23.5)	2.92 (23.5)
6.45	4.54 (23.5)	3.01 (23.3)
	4.44 (20.7)	2.92 (23.0)
7.45	4.54 (22.9)	3.00 (23.2)
	4.44 (23.1)	2.92 (23.2)
8.41	4.54 (23.3)	3.00 (23.2)
	4.54 (23.2)	2.92 (23.3)

[a] pH-meter reading is corrected according to ref 18. [b] Appeared as a broad signal. [c] Coupling constants are based on separations between resonances 1,3; 2,4; 5,7; and 6,8 in the sets of doublets C and D. Resonances are numbered starting with the most downfield signal as peak 1 proceeding upfield to peak 8 within the two sets of doublets designated C and D in Figure 1a.

Table II. Rate Data for the Reactions of Uridine Nucleotides with *cis*-Platin at 40 °C, pH = 6.5, and μ = 0.5 M $NaClO_4$

[Pt], mM	[Nucleotide], mM	10^4k_0,[a] s^{-1}	10^6k_1,[b] s^{-1}
	Uridine Diphosphate		
1.6	3.5	1.6 ± 0.2	6.8 ± 0.6
0.5	5.0	1.7 ± 0.2	6.5 ± 0.6
7.5	15.0	1.5 ± 0.1[c]	
	Uridine Triphosphate		
1.2	2.5	1.5 ± 0.2	3.5 ± 0.5
4.7	9.6	1.6 ± 0.2	3.2 ± 0.5
0.5	5.0	1.6 ± 0.2	4.3 ± 0.5
5.0	15.0	1.4 ± 0.1[c]	

[a] Rate constant for the initial phase of the reaction; average values for at least three kinetic runs. [b] Rate constant for the final phase of the reaction; average values for at least three kinetic runs. [c] Calculated from ^{31}P intensity data.

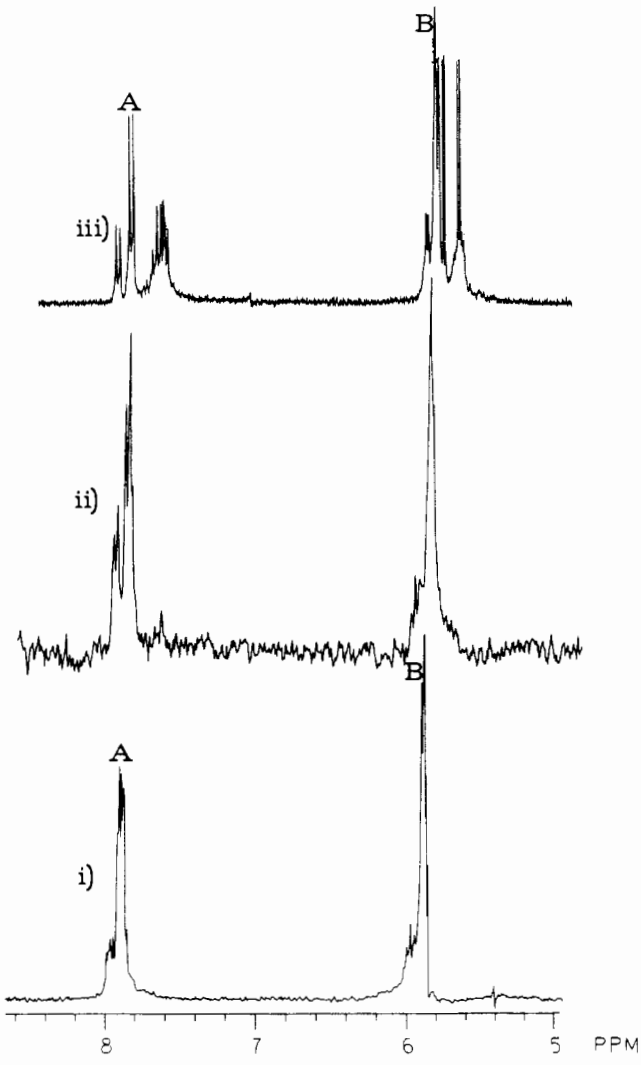

Figure 2. Proton NMR spectra (pyrimidine base protons only) of the UDP (8.0 mM)–*cis*-DDP (16 mM) reaction mixture recorded at (i) 3 h, (ii) 24 h, and (iii) 14 days. Peaks A and B are for the H(6) and H(5) resonances for the free nucleotide, and other signals are for the formation of UDP products.

an analytical column, this microscale separation did not provide sufficient material to allow a characterization of these complexes.

Figure 3 exhibits the HPLC separation of products for the UDP reaction on a C-18 reversed phase column utilizing phosphate buffer (pH = 6.8). Peak A represents the excess unreacted material and peak E is from a UMP impurity. The retention times for A and E correspond to the retention times for free UDP and UMP which were used as standards. Products peaks are labeled as B, C, and D. Two products with longer retention times, C and D, must be less polar while the other product, B is more polar than the free nucleotide. The nitrogen-coordinated products increase the acidity constants of the phosphate groups slightly, and therefore these products are expected to be more polar at pH values below which the completely deprotonated forms exist. On the other hand, phosphate complexation would lead to the decrease in charge of the bound nucleotides. These compounds are expected to be less polar than the free materials. Thus the longest retained fractions are the phosphato complexes. Similar separations were achieved with formate and acetate buffers. Unfortunately, the phosphato complexes suffer faster decomposition in these acidic buffers. The decomposition leads to the formation of free nucleotide which was detected by ^{31}P spectroscopy. This decomposition is not related to the coordinating ability of the mobile phase, since no significant change in the decomposition rate was observed between formate ($HCOOH/HCOO^-$) and phosphate ($H_3PO_4/H_2PO_4^-$) buffers at pH 3.3.

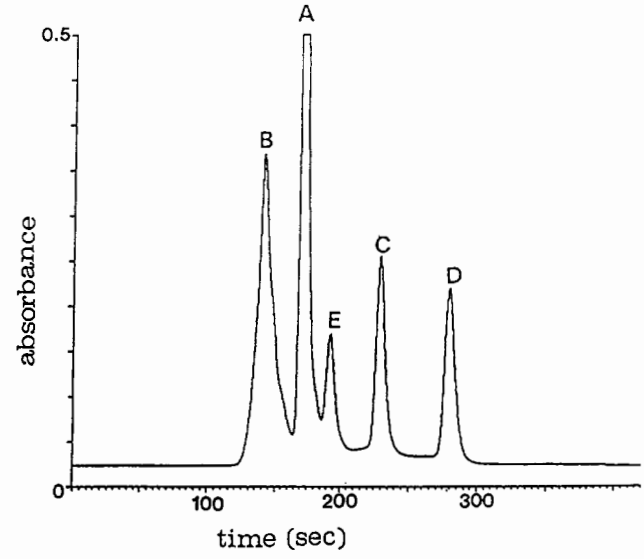

Figure 3. HPLC profile for the *cis*-platin–UDP reaction mixture as in Figure 1a after 24 h on a C-18 column. Peak A is for free UDP, peak B is for nitrogen bound complex, peaks C and D are for phosphato diastereomers, and peak E is the UMP impurity. Phosphate buffer (pH 6.8, 0.5 M) was utilized as mobile phase with a 1 mL/min flow rate.

Although these mobile phases are known to coordinate, ^{31}P NMR spectra did not reveal peaks for orthophosphatoplatinum(II) complexes when phosphate buffer was added to the reaction mixture at the end of the reaction. Similarly, sodium formate at pH 8.0 did not displace the coordinated UDP, as no change in the ^{31}P spectra were observed upon the addition of formate.

The CD spectrum of the fraction C exhibits a very small shoulder at 300 nm ($[\theta] = 0.9 \times 10^2$ deg M^{-1} cm^{-1}) and a relatively large positive Cotton effect at 260 nm ($[\theta] = 1.1 \times 10^3$ deg M^{-1} cm^{-1}). A small negative Cotton effect appeared at 300 nm ($[\theta] = 1.0 \times 10^2$ deg M^{-1} cm^{-1}) for the complex D. The same fraction also showed a comparable positive Cotton effect at 260 nm ($[\theta] = 1.1 \times 10^3$ deg M^{-1} cm^{-1}) as observed for complex C. The estimated concentrations for the phosphato complexes which were determined spectrophotometrically ranged from 3.2×10^{-5} M for fraction C to 1.4×10^{-5} M for fraction D in about 0.5 mL of eluate upon injection of 10 μL in the column. In order to ascertain whether a peak exists at 300 nm for complex C, higher concentrations for the reaction mixtures were subjected to HPLC separations. Unfortunately, both peaks C and D in the chromatogram were significantly broadened and appeared as overlapped peaks. Circular dichroism spectra of the poorly resolved fractions did not add any further information at 300 nm.

Following the HPLC separation, each fraction representing the phosphato complex was collected and reinjected into the column at various time intervals. Figure 4 shows that each product redistributes to a mixture of these complexes in 1.5 h and that the phosphato complexes suffer decomposition with the release of some free UDP. The equilibration did not yield equally intense signals nor did the original mixture exhibit the equal intensity. Complex C is slightly more abundant (assuming that both the complexes have equal molar absorptivity) over the complex D. However, there is no significant difference in the half-life of equilibration for these isomers. A half-life of 25 ± 5 min can be estimated from the intensity-time data (Table III).

Reaction of UTP with *cis*-DDP. The reaction of UTP with the platinum complex was also followed by NMR and UV–vis spectroscopy. Like the UDP reaction, this reaction also takes place in two distinct phases. The initial phase of the reaction (20 h at pH 6.5) is associated with the formation of phosphato chelates and nitrogen bound products. The final phase of the reaction is accompanied by the appearence of a purple color in 15–21 days at pH 6.5. Figure 5a shows the phosphorus-31 resonances of the

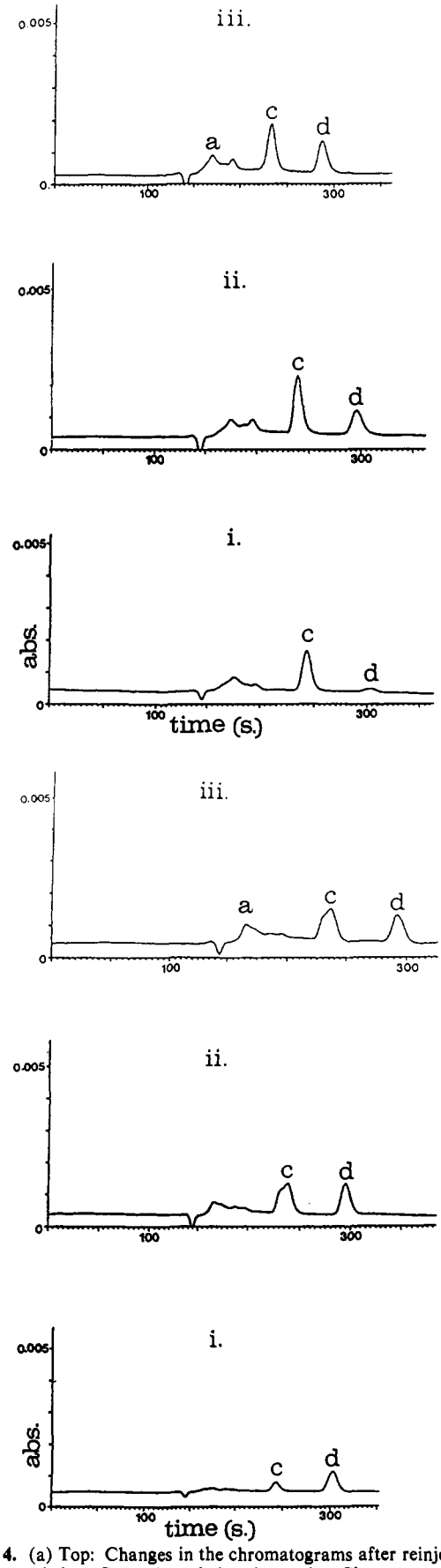

Figure 4. (a) Top: Changes in the chromatograms after reinjection of phosphato chelate C at selected time intervals. Chromatograms i–iii were recorded 15, 65, and 95 min after collection of pure C. Other conditions were exactly the same as in Figure 3. (b) Bottom: Changes in chromatograms after reinjection of phosphato chelate D. Chromatograms i–iii were recorded 15, 65, and 95 min after collection of pure D. Other conditions were the same as in Figure 3.

Table III. Variation of HPLC Peak Intensities[a] Diastereomeric Platinum(II)–UDP Phosphato Complexes with Time

	redistribution of peak c			redistribution of peak d		
time,[b] min	peak c	peak d	hydrolyzed[c] peaks	peak c	peak d	hydrolyzed[c] peaks
0	1.0				1.0	
15	0.8	<0.05	0.2	<0.1	0.9	<0.1
40	0.6	0.1	0.3	0.3	0.6	0.1
65	0.5	0.2	0.3	0.4	0.4	0.2
80	0.4	0.3	0.3	0.4	0.4	0.2
95	0.4	0.3	0.3	0.4	0.3	0.3
135	0.4	0.3	0.3	0.4	0.3	0.3

[a] See the caption for Figure 4a,b for peak designations. [b] Time zero represents the instant when pure c or d was collected from the HPLC column. [c] Combined intensities of two small peaks deisgnated as "a" in Figure 4a,b.

Table IV. Phosphorus-31 Chemical Shifts (Coupling Constants) of Pt(II)–UTP Phosphato Complexes of as a Function of pH

	Chemical Shifts, ppm	
pH[a]	γ-phosphate multiplet,[b,d] F	β-phosphate doublet of doublet,[c,d] G
2.50	2.63	–8.64[b]
3.40	3.88	–8.77[b]
4.38	4.06	–8.89 (22.5)[e]
5.48	4.11	–8.83 (18.1)[e]
6.45	4.11	–8.83 (16.9)[e]
7.42	4.17	–8.84 (14.0)[e]
8.65	4.12	–8.89 (17.2) (13.7)
9.45	4.17	–8.86 (16.8) (12.8)

[a] pH-meter reading is corrected according to ref 18. [b] Appeared as a broad signal. [c] Coupling constants are in Hz. [d] The downfield multiplet, F, and the doublet of doublets, G, are labeled according to Figure 2a. [e] Average coupling constant.

reaction mixture at the end of the reaction. The formation of the phosphato complexes is evidenced by the appearance of a broad multiplet (F) and doublets of doublet (G) at about 8 and 10 ppm downfield from resonances of the free nucleotide. Like the UDP system, no further changes in the intensity of these resonances were apparent after 20 h. The broad multiplet (F) exhibits connectivity with the doublets of doublet (G) in the UTP products (Figure 5b). The coordination chemical shifts, COSY connectivity, and splitting patterns indicate that multiplet, F and doublets of doublet, G are for γ- and β-phosphate groups which are coordinated to platinum in a chelate mode. The doublet for the α-phosphate in the β-, γ-chelate is likely to be unaffected and may be masked under the doublet of the free nucleotide. A connectivity between the α-(I) and β-(G) phosphate is not resolved since these signals appear as overlapping peaks and a large contour engulfing the entire area is apparent in the Figure 5b. Phosphorus-31 chemical shifts as a function of pH are tabulated in Table IV.

Like the UDP products, two diasteromers are expected due the creation of an asymmetric center at the β-phosphate group. HPLC chromatograms of the reaction mixture exhibit two peaks, which are the most retained in the column with almost equal intensity and similar retention times. By extension of the arguments presented for the UDP reactions, these two products can be assigned to the diastereomeric chelates. The nitrogen bound product(s) was eluted before the free nucleotide. In addition, UMP and UDP are detected as an impurity, and as the hydrolyzed product. Although, remarkable similarites exist in the chromatograms of the UDP and UTP products, the intensity ratio of the phosphate to nitrogen bound complexes (0.2) is much smaller for the latter nucleotide. The other major difference is that the secondary reaction lead to the formation of purple products instead of blue. This purple complex exhibits a broad band at 500 nm. However, like the UDP system, the intensity of this band largely depends on the nucleotide/platinum ratio, and pH. The band appears to be most intense at equimolar (8

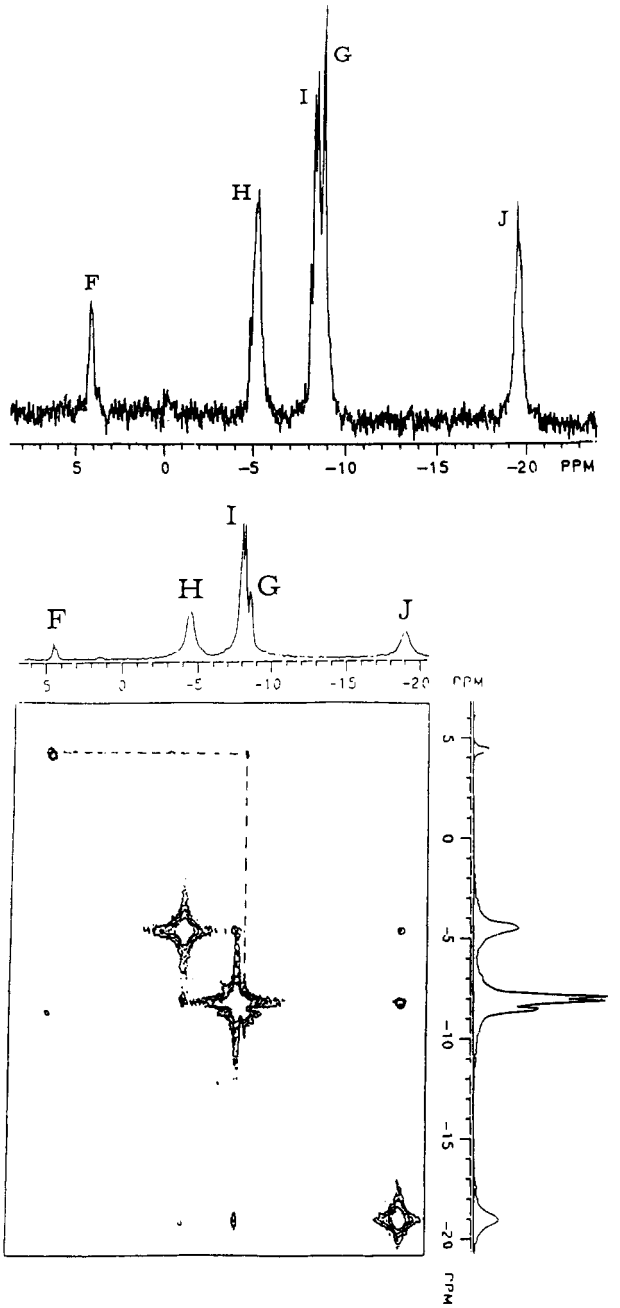

Figure 5. (a) Top: 126.5-MHz phosphorus-31 NMR spectrum of the *cis*-platin (8.0 mM) and UTP (20.0 mM) reaction mixture at pH 7.0 after 18 h. Peaks F and G are for γ- and β-phosphates of the phosphato complexes and peaks H, I, and J are for the γ-, α-, and β-phosphates of free UTP and for the nitrogen bound UTP complexes. (b) Bottom: 2D-COSY ^{31}P spectra of the reaction mixture as in Figure 5a. The connectivity between peaks F and G is indicated by a solid line.

mM) concentration of the reactants and at pH values of about 5. Attempts to separate the purple products by various chromatographic techniques were also unsuccessful, as was observed in the UDP reaction.

The rate constants evaluated from from the absorbance–time and from the ^{31}P NMR data are also listed in Table II. A typical absorbance–time trace along with the computer simulation[19a] is exhibited in Figure 6. The rate constant for the initial phase of the reaction does not depend on the concentration of the nucleotide, and the magnitude of this constant is the same as that found for the UDP reaction.

The acidity constants of the phosphato complexes were estimated from ^{31}P chemical shift–pH data. The chemical shifts of these complexes vary with pH at low pH values. However, no further changes were observed above pH 6, indicating that these

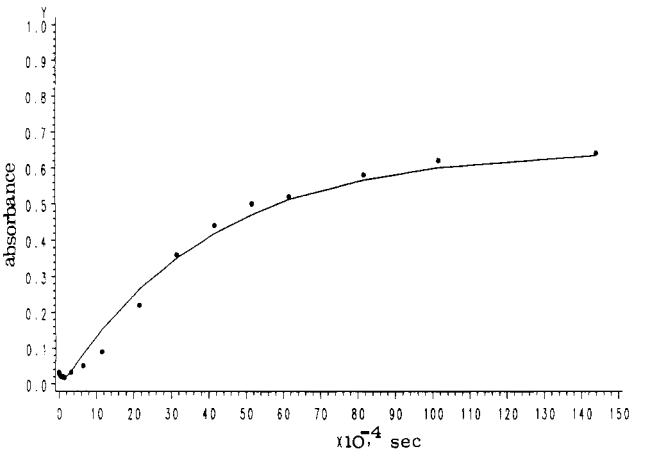

Figure 6. Absorbance change at 375 nm during the reaction between UTP (2.5 mM) and *cis*-DDP (1.2 mM). The solid lines are computer simulated curves according to eq 1 using $k_0 = 1.5 \times 10^{-4}$ s^{-1} and $k_1 = 3.2 \times 10^{-6}$ s^{-1}.

complexes are completely deprotonated above this pH value. Although limiting values of chemical shifts were achieved at higher pH, we were unable to determine chemical shifts for the completely protonated forms owing to a faster decomposition of these complexes below pH 3. However, estimates of the acidity constants were made by utilizing the values of the deprotonated forms through an iterative nonlinear least-squares computer program assuming a monoprotic acid. As can be seen in Table V, the predicted chemical shifts for the protonated forms are substantially lower than experimentally accessible values; therefore, a relatively large uncertainty exists in the reported pK values.

Discussion

The rate constants evaluated from the NMR and UV–vis measurements for the initial phase of the reaction are in good agreement with the rate constant for the aquation of *cis*-DDP.[4,17b] Further, the rate constants do not vary with the nucleotide concentrations. Therefore, the formation of phosphato products in the initial phase of the reaction is primarily limited by the aquation reaction. The new ^{31}P resonances exhibit 8–12 ppm coordination chemical shifts for the bound phosphate groups. These large coordination chemical shifts, spilitting patterns, COSY connectivity, and HPLC and CD data are consistent with the formation of diastereomeric phosphato chelates.[5,17] The nitrogen bound complexes are also formed by the rate limiting aquation process, since the rate data obtained from the UV–vis measurements do not differ from those obtained from ^{31}P intensity measurements. The former measurements are noncommittal for the formation of the products, but the latter is specific to the rate of the formation of phosphato complexes. Some of the nitrogen bound species in the initial reaction further undergo transformation to form blue (UDP) or purple (UTP) products. The mechanisms of formation of the intermediate and products are represented in Scheme I, where P-Nuc = phosphato bound

(19) (a) A reviewer noted that experimental data in the time domain 6.5×10^4 to 6.0×10^5 s in Figure 6 deviate significantly from the calculated values. This is primarily due to the fact that a small and a large change in absorbance are associated with the initial and final phase of the reaction. A small uncertainty in the molar absorptivity of the blue products in the final phase of the reaction reflects a significant deviation in the time domain stated above. Other kinetic schemes including a first-order formation of intermediate followed by a second-order decomposition of the same did not yield kinetic curves which are comparable to the experimental ones. (b) A firm commitment regarding the nature of the initial N(3) bound species can not be made from our data. However, HPLC separations indicate that the amount of unreacted nucleotide present is more than what is expected based on the bis-(N3) complex, taking into account 1:1 phosphate complex formation.

Table V. Observed and Calculated Chemical Shift Data for Pt(II)-UDP and PT(II)-UTP Phosphato Complexes

	chem Shifts, ppm		
pH[a]	obsd	calcd	pK_a
	UDP Complexes		
	β-Phosphate Peaks[b] 1, 3		
2.50	3.15	3.15	2.2[c,d]
3.36	4.27	4.27	
4.40	4.49	4.51	
5.45	4.53	4.54	
6.45	4.54	4.54	
	β-Phosphate Peaks[b] 2, 4		
2.50	3.10	3.10	2.3[e,f]
3.36	4.16	4.16	
4.40	4.41	4.41	
5.45	4.43	4.44	
6.45	4.45	4.44	
	UTP Complexes		
	γ-Phosphate, Multiplet[g-i]		
2.50	2.63	2.63	2.3
3.40	3.88	3.88	
4.38	4.06	4.08	
5.48	4.11	4.11	
6.45	4.11	4.11	

[a] pH is corrected as stated in Table I. [b] Abbreviations are the same as in Table I. [c] Calculated chemical shift for the protonated form is 0.51 ppm. [d] A lower pK_a value, 1.7 was obtained from similar calculations utilizing peaks 5, 7. [e] Calculated chemical shift for the protonated form is 1.05 ppm. [f] A lower pKa value, 1.6 was obtained from similar calculations utilizing peaks 6, 8. [g] Abbreviations are the same as in Table IV. [h] Calculated chemical shift for the protonated form is 0.15 ppm. [i] The doublets of doublet were not used in this calculation because of very small changes in chemical shift (≤0.2 ppm) over the pH range 2.5–8.6.

Scheme I

$$PtCl_2(NH_3)_2 \xrightarrow{k_a} PtCl(NH_3)_2(H_2O)^+ + Cl^-$$

$$PtCl(NH_3)_2(H_2O)^+ + \text{Nucleotide} \xrightarrow{\text{fast}} Pt(\text{P–Nuc})(NH_3)_2 + H_2O + Cl^-$$

$$\xrightarrow{\text{fast}} Pt(\text{N–Nuc})(NH_3)_2 + H_2O + Cl^-$$

$$Pt(\text{N–Nuc})(NH_3)_2 \xrightarrow{\text{slow}(t_{1/2} = 2\text{–}3 \text{ days})} \text{Pt blues/Pt purples}$$

complexes and N-Nuc = nitrogen bound complexes. The charges are omitted for these complexes.

Simultaneous formation of phosphate and nitrogen bound complexes[19b] indicates that the rates of formation of these complexes through the aquated species are comparable. Taking the integrated HPLC intensity data and assuming that the molar absorptivity at 254 nm of the phosphate and nitrogen bound complexes of the nucleotides are similar, the rate ratio, $k_{\text{nitrogen}}/k_{\text{phosphate}}$, is calculated to be 0.8 for the UDP system. However, the absolute magnitudes of the rate constants are not known since the reactions between the aquated complex and nucleotides are not rate limiting processes.

According to the nomenclature presented by Cornelius and Cleland,[20] these phosphato complexes of nucleoside 5′-di- and -triphosphates are (Δ) and (Λ) isomers. Unfortunately, NMR, HPLC, and CD data can not establish the absolute configuration of these isomers. One of the isomers is more stable than the other, as evidenced by the ratio of the of the peak areas in the chromatograms. Also, a small amount of nucleotide is released during this isomerization. The implication is that an aquation leading to the cleavage of a Pt–O bond to form a monodentate phosphato complex may be the rate limiting step for this isomerization process (Scheme II). Once such a monodentate complex is formed, competing processes can lead to formation of

Scheme II

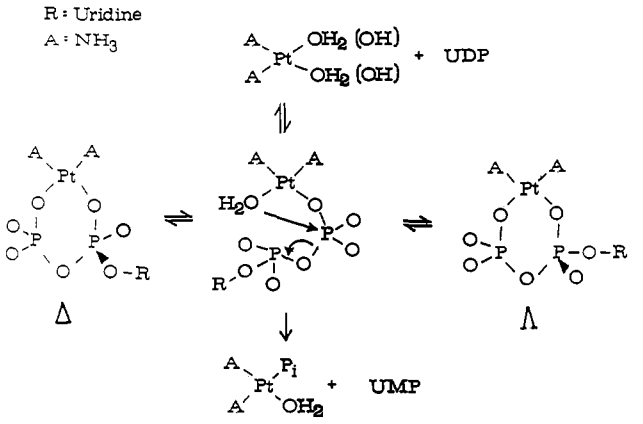

the phosphato complexes (ring closure), and further aquation can proceed to release free UDP. This mechanism is also supported by the fact that in the presence of added UDP no appreciable increase in the free nucleotide concentration, or decrease in the intensity of the ^{31}P signals of diastereomers, was observed over several days. The presence of excess nucleotide is not expected to favor the equilibrium that leads to the formation of free ligand. Furthermore, when the phosphato complexes are separated, utilizing either acetate or formate buffer, followed by the ^{31}P measurements (1–2-h experiment) all of the resonances that are observed correspond to the free nucleotide. These observations are also consistent with the fact that the platinum(II) substitution reaction is acid-catalyzed and that at lower pH the phosphate groups are protonated and therefore ring closure is not favorable over the deligation.

The higher stability of one isomer over the other is likely to be related to the specific interactions of the uncoordinated phosphate oxygen with the coordinated ammine ligands and the interaction with the remainder of the nucleotide structure. The configurations of Rh(III)–ATP complexes have been established by comparing the activities of Co(III) and Cr(III) analogs toward a wide variety of enzymes. For examples, Cleland and coworkers[21] demonstrated that for Co(III) and Cr(III) complexes, the (Λ) isomers are active toward argenine kinase, creatine kinase, glycerokinase, hexokinase, glutamine synthetase, and Mg–ATPase, while the (Δ) isomer is the substrate for pyruvate kinase, myokinase, phosphofructokinase, protein kinase, Na,K–ATPase, and Ca–ATPase. Unfortunately, we can not take advantage of this structure–activity relationship in our system since UTP is not a substrate toward these enzymes. Once the enzymatic activities toward Co(III)–UTP complexes of known configurations are investigated, they would be helpful in inferring the configurations of these UTP complexes.

Returning now to the blue and purple products formed in the secondary reaction, it appears that platinum is most likely coordinated to the nitrogen and the exocyclic oxygens of the pyrimidine base in these complexes. Since no changes in intensity or coupling patterns were observed in the ^{31}P signals of the phosphato complexes, formation of oligomeric platinum phosphato blues can be ruled out. Although platinum phosphate blues are reported,[17b,22,23] ^{31}P signals of these blues are much broader[23,24] than what has been observed here, and the chemical shifts of these blues are markedly different from those for monomeric platinum(II) complexes.[24] The platinum–UDP blue is perhaps

(20) Meritt, E. A.; Sundaralingam, M.; Cornelius, R. D.; Cleland, W. W. *Biochemistry* **1978**, *17*, 3274.

(21) Cleland, W. W. In *Mechanisms of Enzymatic Reactions: Stereochemistry*; Frey, P. A., Ed.; Elsevier: New York, 1985.

(22) Appleton, T. G.; Berry, R. D.; Hall, J. R. *Inorg. Chim. Acta* **1982**, *64*, 229–233.

(23) Wood, F. E.; Hunt, C. T.; Balch, A. L. *Inorg. Chim. Acta* **1982**, *67*, 19–20.

(24) Bose, R. N.; Viola, R. E.; Cornelius, R. D. *Inorg. Chem.* **1984**, *23*, 1181–1182; **1985**, *24*, 3989–3996.

similar to those observed for platinum–uracil and platinum–α-pyridone blues by Lippard and co-workers.[25] These workers have established that platinum blues, containing a variety of amide ligands, are mixed valence tetramers in which two bridged dimeric units are held by a weak Pt–Pt bond. The average oxidation state of platinum in these blues is +2.25. X-ray structural characterization of the platinum 1-methyl uracil blue[25c] reveals that two platinum dimers with bridged uracil through N3 and O4 are held by a weak Pt–Pt bond. The upfield chemical shift of H6 proton in the "blue and purple" is in accord with the bridging nitrogen and oxygen of the pyrimidine base reported by Lippert and co-workers.[28] The purple complex in the UTP reaction is analogous to that observed for 1-methylthymine complex.[29] On the basis of oxidation by Ce^{4+}, the average oxidation state of platinum was formulated as +3.75 in this complex. However, the assignment of this oxidation state has been questioned by Renn and Lippert.[28] On the basis of XPS studies on blues, these authors[28] concluded that the oxidation state of the purple complexes should lie between 2 and 3. Since the minor UDP blue and UTP purple complexes have not yet been isolated from solution, it remains to be seen whether these blue and purple complexes are structurally similar to those reported earlier.[25,28,29]

Acknowledgment. Funding of this research by the National Institutes of Health (Grant GM 40006) is gratefully acknowledged. We also thank Professor Roger Gilpin for access to his CD spectrophotometer. We are thankful to Johnson Mathey, Inc., for the generous loan of K_2PtCl_4.

(25) (a) Barton, J. K.; Caravana, C.; Lippard, S. J. *J. Am. Chem. Soc.* **1979**, *101*, 7269; Barton, J. K.; Lippard, S. J. *Ann. N.Y. Acad. Sci.* **1978**, *313*, 686. (b) Hollis, L. S., Lippard, S. J. *J. Am. Chem. Soc.* **1983**, *105*, 3494–3503. (c) Mascharak, P. K.; Williams, I. D.; Lippard, S. J. *J. Am. Chem. Soc.* **1984**, *106*, 6428–6430.
(26) Slavin, L. L. Ph.D. Thesis, Kent State University, 1992.
(27) Goodgame, D. M. L.; Jeeves, I. *Z. Naturforsch.* **1979**, *34C*, 1287–1288.
(28) Renn, O.; Lippert, B. *Inorg. Chim. Acta* **1990**, *167*, 123–130.
(29) Thomson, A. J.; Roos, I. A. G.; Graham, R. D. *J. Clin. Hematol. Oncol.* **1977**, *7*, 242.